Adsorption of polycyclic aromatic hydrocarbons at the air-water interface: Molecular dynamics simulations and experimental atmospheric observations

Robert Vácha,[a] Pavel Jungwirth,[a] Jing Chen,[b] and Kalliat Valsaraj[b*]*

[a]*Institute of Organic Chemistry and Biochemistry, Academy of Sciences of the Czech Republic, and Center for Biomolecules and Complex Molecular Systems, Flemingovo nám. 2, 16610 Prague 6, Czech Republic*

[b]*Cain Department of Chemical Engineering, Louisiana State University, Baton Rouge, LA 70803-7303, USA*

[*]*Corresponding authors: pavel.jungwirth@uochb.cas.cz (P. J.) and valsaraj@lsu.edu (K. V.)*

Abstract

Adsorption of benzene, naphtalene, anthracene, and phenanthrene at the aqueous surface is investigated by means of molecular dynamics simulations. Potentials of mean force, i.e., free energy profiles of moving the studied molecules across an aqueous slab were evaluated. In all cases, deep surface free energy minima, corresponding to orders of magnitude of surface enhancement of the aromatic molecule, were located. This enhancement, which increases with the size of the solute, points to the importance of the aqueous surface for the chemistry of polycyclic aromatic hydrocarbons (PAHs). Supporting evidence in the atmospheric environment related to the heterogeneous chemistry of PAHs on water droplets and planar surfaces is summarized. There is good agreement between the hydration free energies computed from MD calculations and the experimentally determined values. Data pertaining to the importance of air/water interface in the adsorption and transport of PAHs on micron sized water droplets are described. The relevant data on adsorption and reaction (ozonation and photochemical) at the air/water interface of planar surfaces and droplets are also summarized.

Introduction

Polycyclic aromatic hydrocarbons (PAHs) belong to a class of organic compounds that is environmentally significant.[1] PAHs comprise of the simplest two-ring compound (naphthalene) and a large number of multi-ring, high molecular weight compounds. N-, O- and S-containing PAH compounds are also known to exist in the environment. PAH compounds exist in the gas phase and adsorb to particulates in the atmospheric environment. They are ubiquitous and arise from a variety of sources including fossil fuel combustion, biomass burning, coal gasification, smelting operations, petroleum cracking, forest fires, volcanic eruptions and even organism biosynthesis. As a special example,[2] the catastrophic collapse of the World Trade Center in New York City on September 11, 2001 produced PAH concentrations in the air as high as 30 $ng.m^{-3}$. Worldwide total PAH concentrations in air vary from 0.01 to 100 $ng.m^{-3}$ and exhibit a linear increase with human population, indicating their anthropogenic origin.[3] Most developing countries show high atmospheric PAH concentrations.

Most of the PAHs have very low vapor pressure but high aqueous activity coefficients and are known to be hydrophobic in nature. As a result, PAH molecules aggregate in organic-rich environments such as sediments, soils, biota, and aerosols. Many of the PAH compounds show carcinogenic, mutagenic, or genotoxic effects in animal experiments. It is also suspected that oxidation products of PAHs in the atmosphere are more toxic and harmful to the biota than the parent molecules.[4,5] Hence, understanding the chemodynamic behavior of PAHs in the environment has become an important topic of research.

PAH compounds in the atmosphere are typically associated with aerosols and their lifetimes can be long. Gas/particle exchange is one of the dominant mechanisms of

transport for PAH molecules. The gas/particle partitioning is dependent on the air temperature, air relative humidity (moisture content), and the nature of solid particles that make up the aerosols. It is becoming increasingly clear that the presence of water can potentially influence the reactivity at the surface of the aerosol and the extent to which it is able to participate in heterogeneous atmospheric reactions. Recent studies indicate that even small amounts of strongly bound surface-adsorbed water may play a critical role in the interaction of gases with surfaces traditionally presumed to be solid. The presence of thin water films, or so-called "adlayers", on particulates in the atmosphere opens up the possibility of reactions occurring on the water surface, via adsorption of reactive gases onto the water film, within the water layer, via dissolution of reactive compounds into the condensed phase, and at the solid/water interface.[6]

The behavior of a gaseous PAH molecule at the air-water interface is important in determining its fate and transport in the environment. Air-water interface exists in different forms: (i) bulk phase contact (e.g. air-sea), (ii) air dispersed in bulk water (e.g., air bubbles in water), (iii) water droplets in bulk air (e.g., fog, mist) and, (iv) thin water films on solids (e.g., water films coating aerosols and water coating soil particles in the unsaturated soil zone). In all these cases, the air-water interfacial area can be large and provides an important venue for adsorption and reaction. Although much is known about the partitioning of PAH molecules between bulk air and water phases, much less in known about the adsorptive behavior at the air-water interface.[7] Only recently has this become a focus of research.[8-13] For example, adsorption parameters for a few PAH molecules have been recently reported.[14] Similarly, a few recent papers have shed light on the reactions occurring between adsorbed PAH molecules and ozone on both planar and highly curved interfaces.[11,12,15-19] In spite of this experimental evidence presented in

the literature, there has been no molecular scale discussion presented on the behavior of PAH molecules at the air-water interface. This paper summarizes our recent work on molecular dynamics simulations of the aqueous solvation of four typical aromatic compounds. We begin with the monocyclic aromatic hydrocarbon (benzene) and then move towards three PAH molecules (naphthalene, anthracene, and phenanthrene). For each species, we have obtained the free energy profile for moving the molecule from the gas phase to the aqueous phase through the air-water interface. The available experimental results are compared to our calculations, and we describe the atmospheric implications of our observations with supporting data.

Systems and Computational Method

We used classical molecular dynamics (MD) simulations for investigation of the aqueous hydration and surface propensity of PAHs. In particular, we employed the program package Gromacs 3.1.5[20] to evaluate the potential of mean force (PMF), i.e., the free energy profile ΔG associated with moving the molecule from the gas phase across the aqueous interface to the liquid bulk and back into the gas phase. From the free energy difference between the two points in the path (e.g., in the liquid, at the surface, or in the gas phase) one can evaluate the molecular concentration ratio of the studied species

$$\frac{\mathbf{c}_1}{\mathbf{c}_2} = \mathbf{e}^{-\frac{\Delta \mathbf{G}_{12}}{\mathbf{RT}}}$$

The hydration free energy is related to the Henry's constant by the state equation of an ideal gas and the above equation. The values of Henry's law constant were taken from a compilation by Sander[21] and were used to verify the quality of employed force-fields. Note that hydration free energy depends on the choice of a standard state, which in

our case is that corresponding to infinite dilution. The solvation free energies at ambient conditions (i.e., p_0 = 1 atm gas pressure and c_0 = 1 M concentration) differ from those corresponding to a single gas molecule (pertinent to the present simulations) by a factor RT ln(RTc_0/p_0) = 1.9 kcal/mol.[22]

Our system consisted of 215 - 430 water molecules and one molecule from the following list: benzene, napthalene, anthracene, and phenanthrene. This system was placed in a prismatic unit cell of dimensions 18.6 x 18.6 x 388 Å (215 water molecules and benzene or naphthalene) or 23.5 x 23.5 x 200 Å (430 water molecules and naphthalene, anthracene, or phenanthrene) and 3D periodic boundary conditions were applied. This results in an extended slab with an aqueous bulk between two air-water interfaces.[23]

We employed the SPC/E model of water.[24] For benzene and the PAHs, we chose among the existing parameterizations (or modifications thereof) those, which reproduced best the experimental hydration free energies. The employed Lennard-Jones parameters are σ = 3.40 Å and ε = 0.086 kcal/mol for carbon and σ = 2.60 Å and ε = 0.015 kcal/mol for hydrogen, which corresponds to values from the standard GAFF force field.[25] The atomic charges were evaluated from an optimized structure with the RESP method after an *ab-initio* HF/6-31g* calculation by fitting the electrostatic potential at points selected according to the Merz-Singh-Kollman scheme. As in our previous study,[23] the employed molecular force field is non-polarizable. This is partly jusstified by the fact that no ions (for which electronic polarization effects were shown to be particularly important[26]) are present and partly by the sizable computational costs of PMF calculations for large solutes. Instead, we somewhat increased the atomic partial charges on the solute in order to account for the averaged polarization effect (and, implicitly, for the aromaticity of the

carbon rings) and to better reproduce the molecular quadrupoles. The multiplication factor for atomic charges was 1.24 for benzene, 1.40 for napthalene, and 1.45 for anthracene and phenanthrene. Note, that even after this increase the partial charges remained relatively small, not exceeding for hydrogen atoms the value of about 0.2 e. An interaction cutoff of 9 Å was applied with long range electrostatic interaction being accounted for using the particle mesh Ewald method.[27]

To calculate the PMF we used an approach based on a shifting harmonic constraint in the direction perpendicular to the surface. This so called z-spring method is described in detail in our previous paper.[23] Very long (nanosecond) equilibration times were required, since we moved large molecules in extended systems with hundreds of water molecules.

Computational Results

Figures 1-4 show for each of the investigated systems the corresponding PMF, which is the free energy profile of moving the PAH molecule through the aqueous slab, i.e., from the gas phase across the air/water interface into the aqueous bulk and across the second interface back into the air. Ideally, these curves should be perfectly symmetric with respect to the center of the slab, and we indeed see very good left-right symmetry, indicating convergence of the free energy profiles.

All the aromatic molecules under study – benzene, napthalene, anthracene, and phenanthrene, are volatile species, with their volatility gradually decreasing with molecular size. Note that in all these cases, the hydration free energy is negative, meaning that the concentration of the molecule is lower in gas phase than in the aqueous bulk. Experimental hydration free energies evaluated from Henry's constants[21] are very well

reproduced for all studied molecules (Figs. 1-4). Note that with the increasing number of aromatic rings the molecules the hydration free energy increased from less than –1 kcal/mol for benzene to more than –4 kcal/mol for phenanthrene.

One significant result of the present calculations is the deep surface minimum at the PMF of benzene and, even more prominently, for the investigated PAHs. Occurrence of such a pronounced minimum is directly reflected in a large surface enhancement of the studied aromatic molecules. This huge surface enhancement, which is clearly a generic feature of benzene and PAHs, is quantified in Table 1. Compared to the gas phase, there is more than two orders of magnitude surface enhancement for benzene, while for phenanthrene it is almost six orders of magnitude. Interestingly, the mean enhancement at the surface with respect to the aqueous bulk is much less system dependent and amounts to roughly a factor of hundred for all investigated molecules. Finally, note that we employed a non-polarizable force-field, which is likely to lead to underestimation of the surface effect. The present results can, therefore, be viewed as a lower estimate to the concentration enhancement of benzene and PAHs at the aqueous surface.

Experimental Observations and Atmospheric Implications

In the literature there exist numerous pieces of experimental evidence in support of the theoretical conclusions reached in the above sections. The free energy minima for the PAH molecules at the air-water interface have several implications for their atmospheric chemistry. In cases where the surface area is large the surface reactivity of PAH molecules can be more significant than the bulk chemistry. Such cases exist for atmospheric droplets, ice, snow, and thin water films on aerosols. Similar situations also exist in water films on solid particles in the unsaturated soil zone, air bubbles in water and

sea salt aerosols. In the following sections, we summarize various findings that pertain to the importance of the air-water interface enrichment of PAHs in the atmospheric environmental context.

Comparison of Free Energies of Adsorption

In a previous work, Raja et al[14] reported the free energy of adsorption of benzene and several PAH molecules at the air-water interface. The procedure used was inverse gas chromatography (IGC) where sub-micron thick water layers were created on a standard gas chromatography packing and the net retention volume of PAH vapors was used to obtain the partition constant to the interface. The procedure was repeated for several different temperatures and the van't Hoff equation was used to obtain the standard free energy, enthalpy and entropy of adsorption.

The partition constant, $K_{\sigma a}$ at any given temperature is related to the overall free energy of adsorption

$$\Delta^{0}_{a\rightarrow\sigma}\mathbf{G} = -\mathbf{RT}\,\ell\mathbf{n}\left(\frac{\mathbf{K}_{\sigma a}}{\delta_0}\right)$$

where δ_0 is a standard surface thickness (= 6 x 10^{-10} m) which is the ratio of the standard state pressure for the gas phase (= 101.325 kPa) and the standard state Kemball-Rideal surface pressure (= 0.06084 $mN.m^{-1}$). The Kemball-Rideal standard state for the surface is the exact equivalent of the 1 atm pressure standard state for the bulk gas phase. The free energy obtained experimentally can be compared to the value predicted from MD simulations given above. Figure 5 is a parity plot where the 1:1 correspondence is shown as the solid line. Note that the computational and experimental values for naphthalene and benzene are in very good agreement, while the value for phenanthrene shows a large

experimental error.

Adsorption and Transport at the Interface

If adsorption at the air-water interface is an important fate process for PAHs in air, transport (short and long-term) on water droplets (fog), ice and snow in the atmosphere can be a dominant pathway. In order to understand this pathway, Raja and Valsaraj[15,28] conducted a series of experiments on benzene and two PAHs (naphthalene and phenanthrene). They used 55 – 182 μm water droplets in a 1 m tall falling droplet reactor into which a gaseous PAH stream was introduced. The droplet contact time in the reactor was of the order of 10 – 50 ms, so that a ratio of the droplet PAH concentration (C_d) to the gas-phase PAH concentration (C_g) at the exit could be determined:

$$\mathbf{K_{DV}}(\tau) = \frac{\mathbf{C_d}}{\mathbf{C_g}} = \zeta \mathbf{K_{wa}} \left[1 - \mathbf{exp}\left(- \mathbf{K_c} \frac{1}{\zeta \mathbf{K_{wa}}} \frac{6}{\mathbf{d_D}} \tau \right) \right]$$

where ζ represents the deviation of the bulk phase partitioning as a result of surface adsorption and is given by $1 + \frac{6}{\mathbf{d_D}} \frac{\mathbf{K_{\sigma a}}}{\mathbf{K_{wa}}}$. Note that ζ of 1 means that surface adsorption effects are neglected and only bulk phase partitioning is assumed. In the above equation, K_c represents the overall mass transfer coefficient of the PAH to the droplet from the gas phase and includes the resistance to gas phase diffusion, mass accommodation to the surface, and the resistance to the liquid phase diffusion. The term d_D represents the average droplet diameter in the reactor. Note that the term in the square brackets in the above equation is the fractional approach to equilibrium.

The above equation shows that if adsorption is dominant then K_{DV} should show a dependence on d_D. This dependence is shown in Figure 6 using the data obtained from

Raja and Valsaraj.[15,28] Firstly, for any given d_D, the droplet-vapor partition constant is in the order benzene < naphthalene < phenanthrene. This is in accord with the MD simulation predictions and the experimental values of the interface partition constants described above. Secondly, there is another important effect shown in this figure. There are two curves: the solid lines showing the predictions with inclusion of the interface partition effects ($\zeta > 1$) and the broken line which considers only bulk phase partitioning and neglects partitioning to the interface ($\zeta = 1$). It is obvious that the latter does not predict the trend at very small droplet diameters. For small droplets, the departure from equilibrium is small, and the effect of $\zeta > 1$ becomes readily apparent. For each compound, there is a clear difference between the two curves; the larger the air/water partition constant for the chemical species, the larger the diameter at which the interface effects become apparent. The overall partition constants increase linearly with $1/d_D$. At very large diameters, the effect of the interface partitioning is unimportant and hence the predictions coincide. Moreover, the larger diameter droplets are clearly mass transfer limited in uptake and hence the partition constants are much lower than equilibrium values.

Adsorption and Reactions at the Interface

The adsorption of PAH molecules at the air-water interface has important consequences as far as their loss processes from the atmosphere are concerned. Several lines of evidence have been presented recently in the literature that concern PAH reactivity at the air/water interface. The first one involves the work of Donaldson and co-workers who have shown that adsorbed anthracene at the air-water interface undergoes transformations via reaction with ozone adsorbed from the gas phase.[18,19] This work is the

first of its kind to provide direct experimental observations of the heterogenous reaction of PAH with an oxidant in the gas phase occurring at the air-water interface of a planar water film. The fluorescence intensity of anthracene was monitored as a function of the ozone concentration and the intensity changes were related to the overall loss rate at the interface.

A Langmuir-Hinshelwood mechanism was proposed that involves simultaneous adsorption of ozone and anthracene at the interface and subsequent reaction between adsorbed molecules (Figure 7). This work was later rationalized for reactions of two other PAH molecules (naphthalene and phenanthrene) with ozone on micron-sized water droplets.[16] The overall rate of oxidation of the PAH (mol.cm^{-2}.s^{-1}) was given by

$$-\mathbf{r}_{\mathbf{PAH}} = \mathbf{k}_{\mathbf{LH}}^{\mathbf{II}}\mathbf{S}_0\theta_{\mathbf{O3}}[\mathbf{PAH}]_{\mathbf{surf}}$$

where θ_{O3} is the surface coverage by ozone molecules, S_0 is the total number of adsorption sites (cm^{-2}) and k_{LH}^{II} is the second order Langmuir-Hinshelwood surface rate constant (cm^2.s^{-1}). $[PAH]_{surf}$ (mol.cm^{-2}) is the surface concentration of PAH on the droplet. The pseudo first-order rate constant, k_s is given by

$$\mathbf{k}_{\mathbf{s}} = \mathbf{k}_{\mathbf{LH}}^{\mathbf{II}}\mathbf{S}_0\theta_{\mathbf{O3}}$$

Note that k_s is primarily determined by $\theta_{O3,}$which is given by the Langmuir equation

$$\theta_{\mathbf{O3}} = \frac{[\mathbf{O}_3]_{\mathbf{surf}}}{[\mathbf{O}_3]_{\mathbf{surf,max}}} = \frac{[\mathbf{O}_3]_{\mathbf{g}}}{\mathbf{C}_{1/2} + [\mathbf{O}_3]_{\mathbf{g}}}$$

where $C_{1/2}$ is the ozone concentration when the surface coverage is 0.5. It is exponentially related to the adsorption energy. Hence

$$\mathbf{k}_{\mathbf{s}} = \frac{\mathbf{k}_{\mathbf{max}}[\mathbf{O}_3]_{\mathbf{g}}}{\mathbf{C}_{1/2} + [\mathbf{O}_3]_{\mathbf{g}}}$$

where $k_{max}= k_{LH}^{II}S_0$. Values of k_{max} and $C_{1/2}$ obtained are shown in Table 2. The

experimental values clearly showed that k_s behaved linearly at low ozone concentrations, but that it reached an asymptotic value at high ozone concentrations indicating saturation effects on the surface.

The same equation was also found to be useful in analyzing the reaction of ozone towards adsorbed naphthalene and phenanthrene on the surface of small water droplets in a falling droplet reactor for which data were presented by Raja and Valsaraj.[16] The values of the Langmuir parameters for the two compounds are also shown in Table 2. The ozone oxidation of both molecules on small micron-sized droplets was found to proceed much faster than on planar surfaces.

The adsorption of compounds at the air-water interface of thin films also has profound effects on their photochemical reactivity in the atmosphere. The primary photochemistry occurs at the surface of thin water films on particles and droplets. A set of experiments was performed recently to study the uptake of a PAH (naphthalene) from the gas phase and the exposure and photooxidation by UVB radiation in a flow reactor on very thin water films (22 to 450 μm).[28] Reaction products were identified and the "global" rate constants were estimated from the data. This experiment revealed some important features related to the importance of air/water interface in heterogeneous chemistry. Although the reaction products observed were similar to the bulk water reactions, the product concentrations were > 50% higher within the thin film under similar initial conditions. In addition, the initial rates of product formation were 46 – 154 % higher in the thin film. This provided a framework for the mechanistic picture shown in Figure 8. Photochemical reactions in the water film occurs by two simultaneous pathways, a homogeneous (bulk water) reaction and a heterogeneous (interface) reaction. Thus, the overall kinetics is given as

$$\mathbf{r}_{P0} = \mathbf{k}_{homo}[\mathbf{PAH}]_{aq} + \mathbf{k}_{het}\frac{[\mathbf{PAH}]_{surf}}{\delta}$$

where k_{homo} and k_{het} are respectively the overall rate constants for homogeneous and heterogeneous reactions, $[PAH]_{aq}$ is the bulk aqueous phase concentration, $[PAH]_{surf}$ is the surface concentration of the PAH and δ is the film thickness. Since the surface and aqueous concentrations are in equilibrium in the semi-batch flow reactor, the concentrations are related through the air-water interface partition constant and the bulk air-water partition constant of the chemical.

$$\mathbf{k}_{tot} = \mathbf{k}_{homo} + \frac{\mathbf{k}_{het}}{\delta}\cdot\frac{\mathbf{K}_{\sigma a}}{\mathbf{K}_{wa}}$$

Figure 9 shows the values of k_{tot} for three film thicknesses. It is clear that as δ increases or as $1/\delta \rightarrow 0$, the value of k_{tot} is determined by k_{homo} which is a constant. The slope of k_{tot} versus $1/\delta$ at large values gives us the values of k_{het} which are listed in Table 3 for the the significant products isolated in the work. The values of k_{het} are approximately an order of magnitude larger on a thin film of 22 μm water layer compared to k_{homo}.

Conclusions

We have investigated the adsorption of benzene and several PAHs (naphtalene, anthracene, and phenanthrene) at aqueous surfaces using molecular dynamics simulations. To this end, we have evaluated free energy profiles of moving the studied molecules across an aqueous slab as potentials of mean force. We have shown computationally that the transfer of PAH molecules from the gas phase to the water surface is connected with a substantial surface enrichments. The MD-simulated hydration free energies are in a satisfactory agreement with experimental data. The effect of surface enrichment at the

air-water interface (which is, compared to the gas phase, of 2-5 orders of magnitude, increasing with the size of the aromatic molecule) has important implications for the atmospheric behavior of PAHs, viz., uptake and reaction, some of which are summarized in this work.

Acknowledgement

Support from the Czech Ministry of Education (grants LC512 and ME644) and from the US-NSF (grants CHE 0431312 and 0209719) is gratefully acknowledged. At LSU the reseach was supported by the US-NSF (grant ATM 0355291).

Tables:

Table 1. Aqueous bulk concentrations and their highest and averaged values in the interfacial region, compared to the gas phase value (normalized to 1.0).

Molecule	Gas Phase	Aqueous bulk	Aqueous surface highest value	Aqueous surface averaged value
Benzene	1.0	3.3	480	250
Naphthalene	1.0	90	16000	7100
Anthracene	1.0	350	285000	120000
Phenanthrene	1.0	550	500000	170000

Table 2. Rates of Reactions of Gas-Phase Ozone with PAHs at Air-Water Interfaces.

Nature of surface	*PAH molecule*	*Reaction parameters*	
		k_{max} / s^{-1}	$C_{1/2}$/molecule.cm^{-3}
Planar surface[18]	Anthracene	2.5×10^{-3}	2.1×10^{14}
92 μm water droplet[15,16,28]	Naphthalene Phenanthrene	303 3.5	1.9×10^{14} 8.9×10^{11}

Table 3. Homogeneous and heterogeneous rate constants for the formation of products at 296 K from naphthalene at the air-water interface of a 22 μm thick water film.

Product	k_{homo}/ min^{-1}	k_{hetero} / min^{-1}
coumarin	3.7×10^{-4}	5.0×10^{-3}
1-naphthol	4.1×10^{-5}	1.5×10^{-3}

Figure captions:

Figure 1: Potential of mean force for moving benzene through an aqueous slab defined via the water density profile. The experimental hydration energies obtained from the Henry's law constants in several measurements are displayed as horizontal lines.[21]

Figure 2: Potential of mean force for moving naphthalene through an aqueous slab defined via the water density profile. The experimental hydration energies obtained from the Henry's law constants in several measurements are displayed as horizontal lines.[21]

Figure 3: Potential of mean force for moving anthracene through an aqueous slab defined via the water density profile. The experimental hydration energies obtained from the Henry's law constants in several measurements are displayed as horizontal lines.[21]

Figure 4: Potential of mean force for moving phenanthrene through an aqueous slab defined via the water density profile. The experimental hydration energies obtained from the Henry's law constants in several measurements are displayed as horizontal lines.[21]

Figure 5: Comparison of the experimental and MD-simulated free energy of adsorption from the gas phase for benzene, naphthalene and phenanthrene. Experimental data obtained from Raja et al[14].

Figure 6: The effect of the size of water droplets on the partitioning of benzene, naphthalene and phenanthrene from the gas phase to droplet phase. Note that the increase in partitioning for small droplets is only simulated when the surface enrichment is considered, i.e. $\zeta > 1$. Experimental data obtained from literature[15,27].

Figure 7: A sketch of the Langmuir-Hinshelwood mechanism of the heterogeneous reaction of gas-phase ozone with adsorbed PAH at the air-water interface as described by Mmereki et al[19].

Figure 8: A mechanistic picture of the homogeneous and heterogeneous photochemical reactions of a gas-phase PAH molecule on a water film.

Figure 9: The overall first-order reaction rate constant for the conversion of naphthalene to various products on a uniform water film of varying thickness. Data taken from literature[28]. Note that as δ decreases there is a substantial increase in the overall rate constant due to the heterogeneous contribution.

Figure 1:

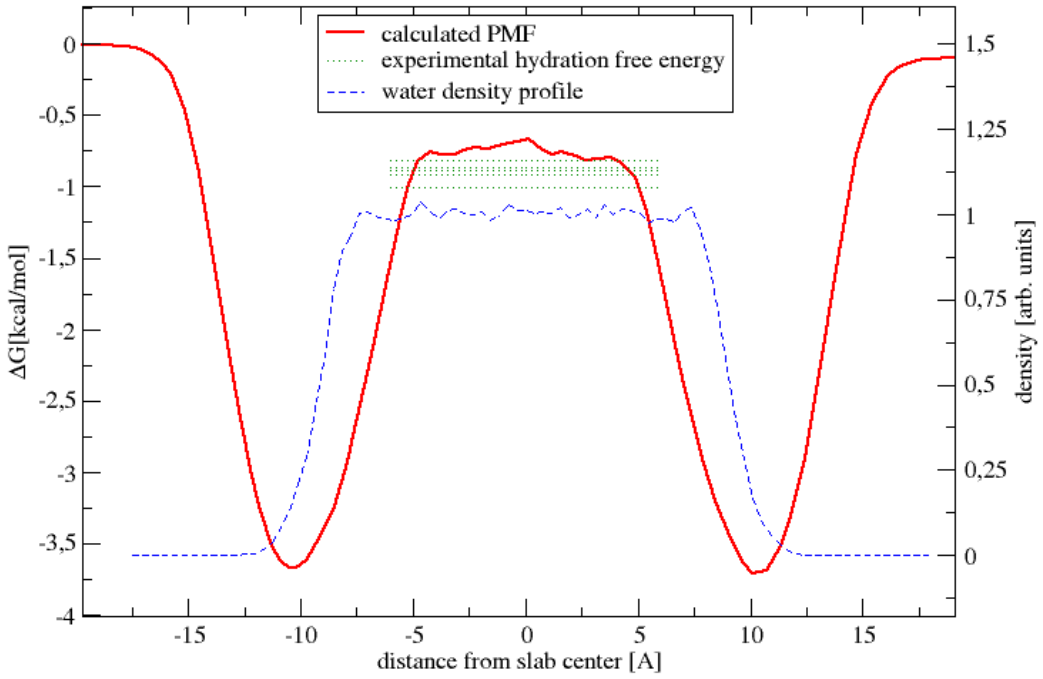
calculated PMF
experimental hydration free energy
water density profile
ΔG[kcal/mol]
density [arb. units]
distance from slab center [A]
0
-0,5
-1
-1,5
-2
-2,5
-3
-3,5
-4
1,5
1,25
1
0,75
0,5
0,25
0
-15
-10
-5
0
5
10
15

Figure 2:

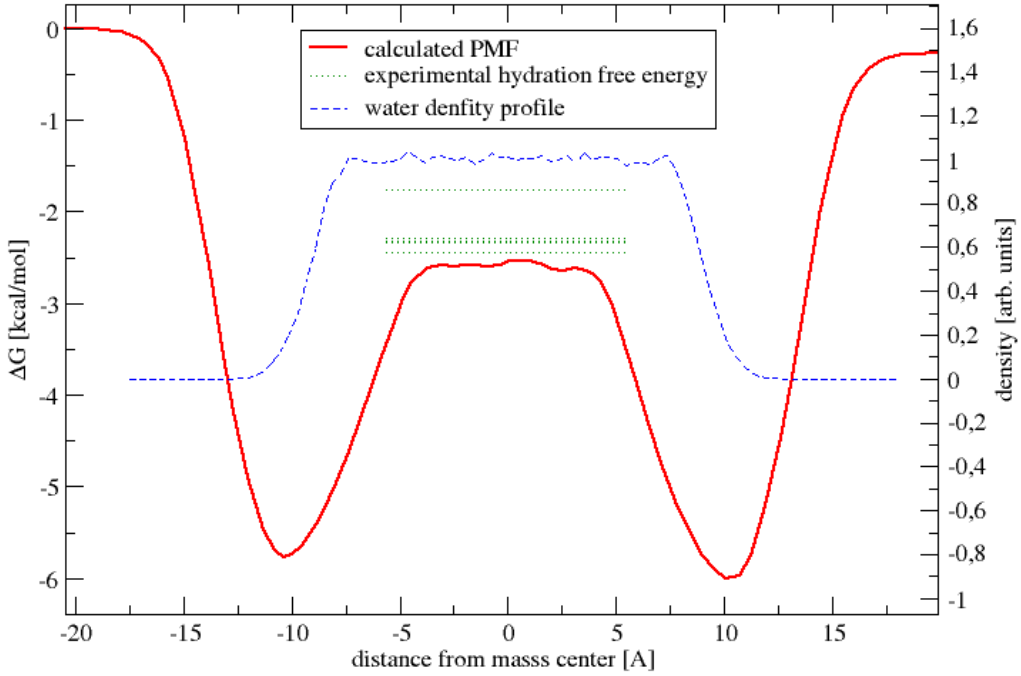
calculated PMF
experimental hydration free energy
water denfity profile
ΔG [kcal/mol]
density [arb. units]
distance from masss center [A]
0
-1
-2
-3
-4
-5
-6
1,6
1,4
1,2
1
0,8
0,6
0,4
0,2
0
-0,2
-0,4
-0,6
-0,8
-1
-20
-15
-10
-5
0
5
10
15

Figure 3:

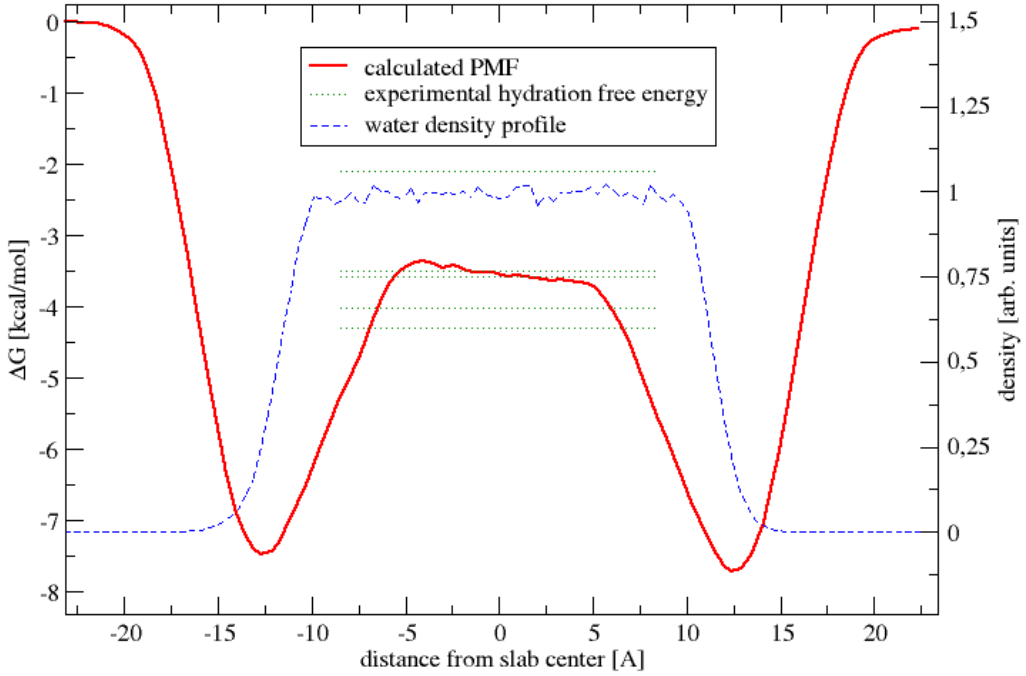
calculated PMF
experimental hydration free energy
water density profile
ΔG [kcal/mol]
density [arb. units]
distance from slab center [A]
0
-1
-2
-3
-4
-5
-6
-7
-8
1,5
1,25
1
0,75
0,5
0,25
0
-20
-15
-10
-5
0
5
10
15
20

Figure 4:

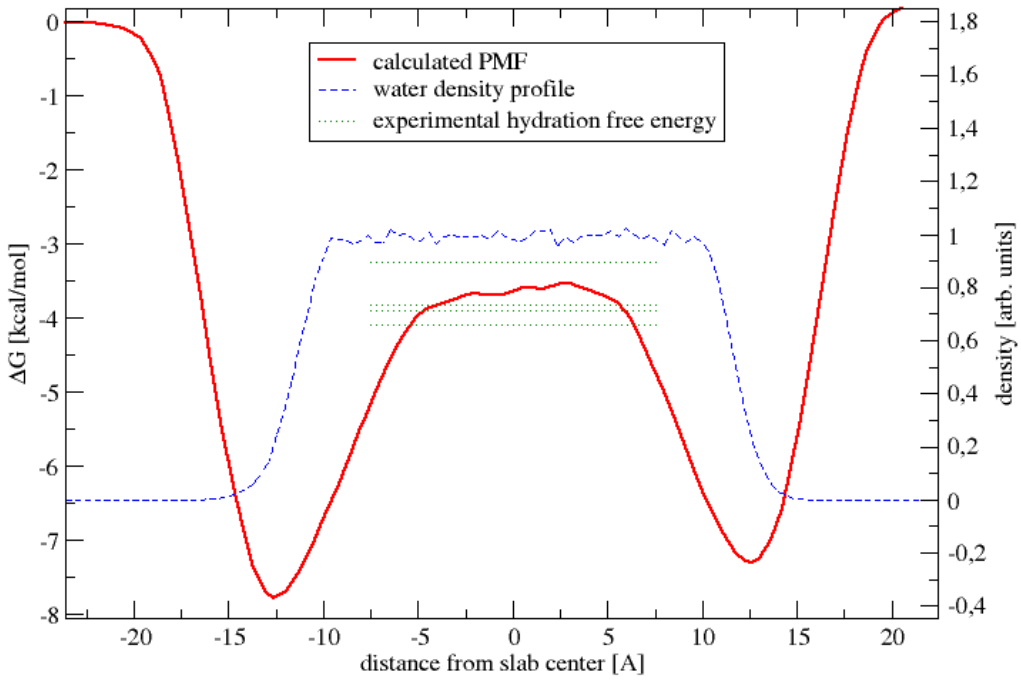
calculated PMF
water density profile
experimental hydration free energy
ΔG [kcal/mol]
density [arb. units]
distance from slab center [A]
0
-1
-2
-3
-4
-5
-6
-7
-8
1,8
1,6
1,4
1,2
1
0,8
0,6
0,4
0,2
0
-0,2
-0,4
-20
-15
-10
-5
0
5
10
15
20

Figure 5:

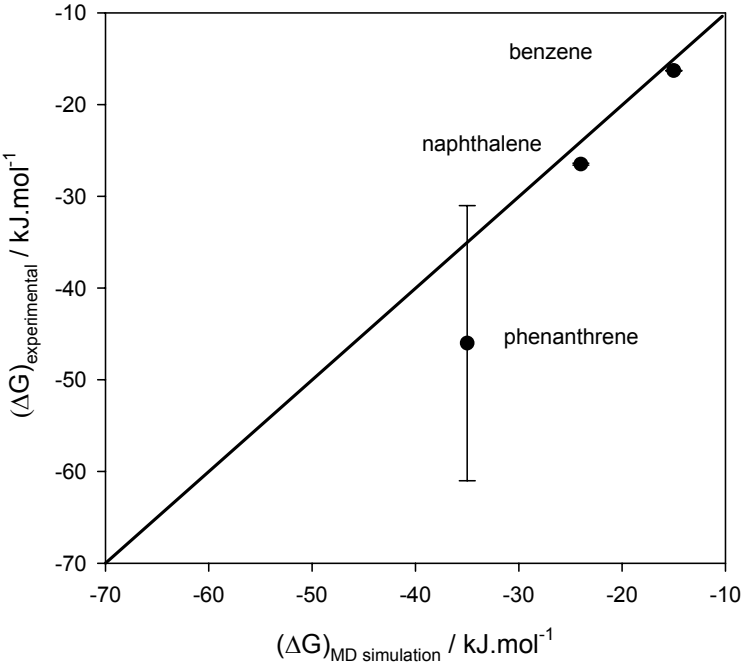
-10
-20
-30
-40
-50
-60
-70
-70
-60
-50
-40
-30
-20
-10
benzene
naphthalene
phenanthrene
(ΔG)experimental / kJ.mol-1
(ΔG)MD simulation / kJ.mol-1

Figure 6:

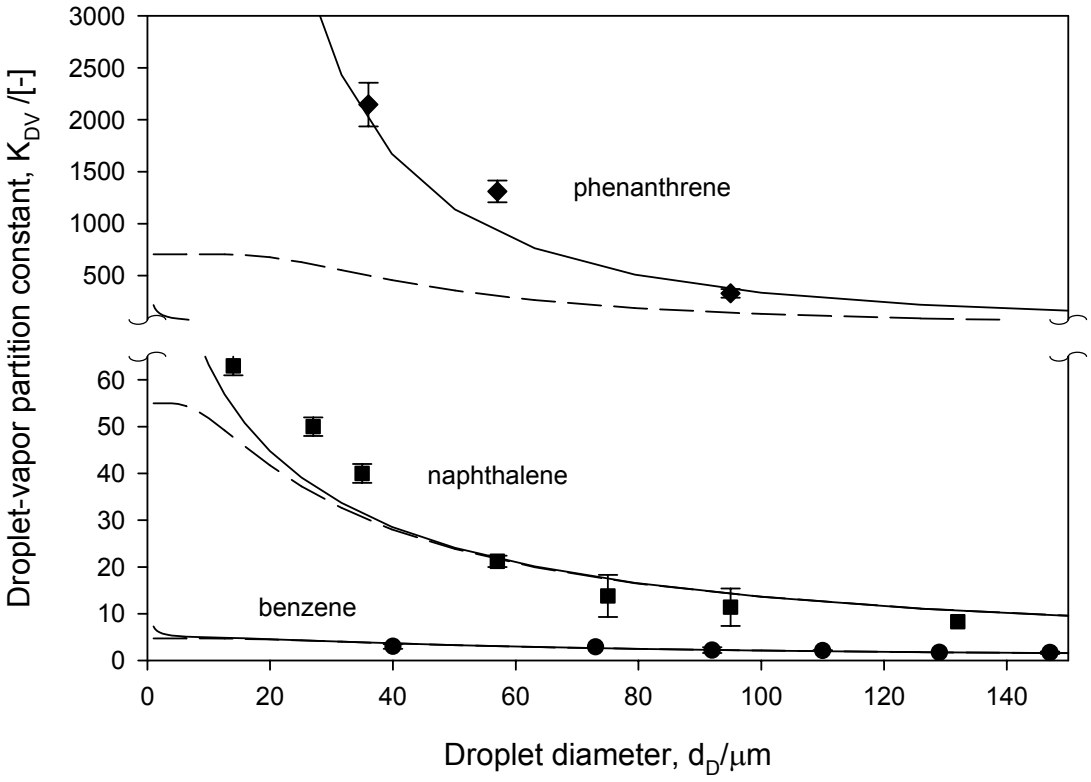
Droplet-vapor partition constant, K_{DV} /[-]
Droplet diameter, d_D/μm
phenanthrene
naphthalene
benzene
3000
2500
2000
1500
1000
500
60
50
40
30
20
10
0
0
20
40
60
80
100
120
140

Figure 7:

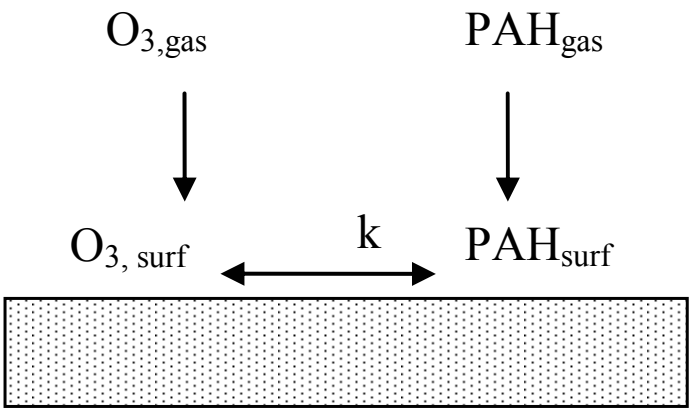

Figure 8:

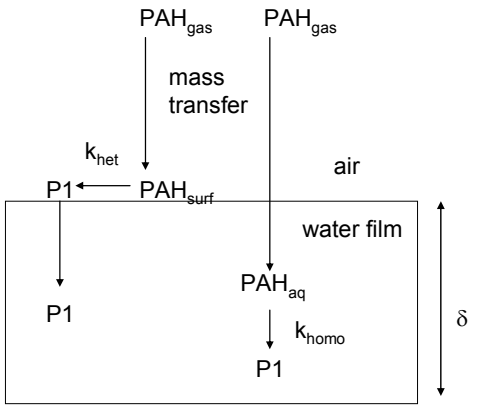

$$\mathbf{k_{tot} = k_{homo}[PAH]_{aq} + k_{het}\frac{[PAH]_{surf}}{\delta}}$$

Figure 9:

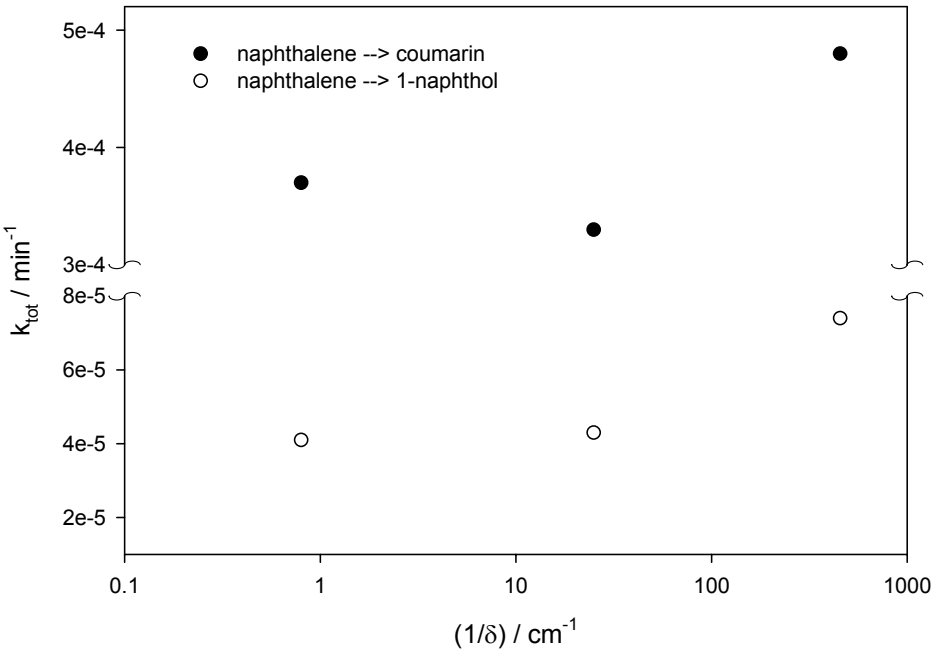
naphthalene --> coumarin
naphthalene --> 1-naphthol
5e-4
4e-4
3e-4
8e-5
6e-5
4e-5
2e-5
k_{tot} / min^{-1}
0.1
1
10
100
1000
(1/δ) / cm^{-1}

References:

(1) Harvey, R. G. *Polycyclic aromatic hydrocarbons*; John Wiley & Sons, Inc.: New York, 1997.

(2) Pleil, J. D.; Vette, A. F.; Johnson, B. A.; Rappaport, S. M. *Proceedings of the National Academy of Sciences of the United States of America* **2004**, *101*, 11685-11688.

(3) Hafner, W. D.; Carlson, D. L.; Hites, R. A. *Environmental Science & Technology* **2005**, *39*, 7374-7379.

(4) *Formation of mutagens from the atmospheric photooxidation of PAH and their occurence in ambient air*; Arey, J.; Atkinson, R.; Harger, W. P.; Helmig, D.; Sasaki, J., Eds.; Statewide Air Pollution Research Center, University of California: Riverside, CA, 1994.

(5) Atkinson, R.; Arey, J. *Environmental Health Perspectives* **1994**, *102*, 117-126.

(6) Sumner, A. L.; Menke, E. J.; Dubowski, Y.; Newberg, J. T.; Penner, R. M.; Hemminger, J. C.; Wingen, L. M.; Brauers, T.; Finlayson-Pitts, B. J. *Physical Chemistry Chemical Physics* **2004**, *6*, 604-613.

(7) Goss, K. U. *Critical Reviews in Environmental Science and Technology* **2004**, *34*, 339-389.

(8) Mmereki, B. T.; Chaudhuri, S. R.; Donaldson, D. J. *Journal of Physical Chemistry A* **2003**, *107*, 2264-2269.

(9) Mmereki, B. T.; Donaldson, D. J. *Physical Chemistry Chemical Physics* **2002**, *4*, 4186-4191.

(10) Mmereki, B. T.; Hicks, J. M.; Donaldson, D. J. *Journal of Physical Chemistry A* **2000**, *104*, 10789-10793.

(11) Donaldson, D. J. *Journal of Physical Chemistry A* **1999**, *103*, 62-70.

(12) Demou, E.; Donaldson, D. J. *Journal of Physical Chemistry A* **2002**, *106*, 982-987.

(13) Donaldson, D. J.; Anderson, D. *Journal of Physical Chemistry A* **1999**, *103*, 871-876.

(14) Raja, S.; Yaccone, F. S.; Ravikrishna, R.; Valsaraj, K. T. *Journal of Chemical and Engineering Data* **2002**, *47*, 1213-1219.

(15) Raja, S.; Valsaraj, K. T. *Environmental Science & Technology* **2004**, *38*, 763-768.

(16) Raja, S.; Valsaraj, K. T. *Journal of the Air & Waste Management Association* **2005**, *55*, 1345-1355.

(17) Donaldson, D. J.; Mmereki, B. T.; Chaudhuri, S. R.; Handley, S.; Oh, M. *Faraday Discussions* **2005**, *130*, 227-239.

(18) Mmereki, B. T.; Donaldson, D. J.; Gilman, J. B.; Eliason, T. L.; Vaida, V. *Atmospheric Environment* **2004**, *38*, 6091-6103.

(19) Mmereki, B. T.; Donaldson, D. J. *Journal of Physical Chemistry A* **2003**, *107*, 11038-11042.

(20) Lindahl, E.; Hess, B.; van der Spoel, D. *Journal of Molecular Modeling* **2001**, *7*, 306-317.

(21) Sander, R. "Compilation of Henry's Law Constants for Inorganic and Organic Species of Potential Importance in Environmental Chemistry (Version 3), www.mpch-mainz.mpg.de/~sander/res/henry.html,", 1999.

(22) Ben Naim, A.; Marcus, Y. *Journal of Chemical Physics* **1984**, *81*, 2016-2027.

(23) Vacha, R.; Slavicek, P.; Mucha, M.; Finlayson-Pitts, B. J.; Jungwirth, P. *Journal of Physical Chemistry A* **2004**, *108*, 11573-11579.

(24) Berendsen, H. J. C.; Grigera, J. R.; Straatsma, T. P. *Journal of Physical Chemistry*

1987, *91*, 6269-6271.

(25) Wang, J. M.; Wolf, R. M.; Caldwell, J. W.; Kollman, P. A.; Case, D. A. *Journal of Computational Chemistry* **2004**, *25*, 1157-1174.

(26) Jungwirth, P.; Tobias, D. J. *Chemical Reviews* **2006**, *106*, 1259-1281.

(27) Essmann, U.; Perera, L.; Berkowitz, M. L.; Darden, T.; Lee, H.; Pedersen, L. G. *Journal of Chemical Physics* **1995**, *103*, 8577-8593.

(28) Chen, J.; Ehrenhauser, F.; Valsaraj, K. T.; Wornat, M. J. *Journal of Physical Chemistry A, in press*.